Mechano-optic regulation of photoconduction in functionalized carbon nanotubes decorated with platinum

C. Mercado-Zúñiga,[1] C. Torres-Torres,[2,*] M. Trejo-Valdez,[3] R. Torres-Martínez,[4] S. Tarrago-Velez,[5] F. Cervantes-Sodi,[5] J. R. Vargas-García[1]

[1]*Depto. Ing. Metalurgia y Materiales, ESIQIE, Instituto Politécnico Nacional, México 07300 D.F., México*

[2]*Sección de Estudios de Posgrado e Investigación, ESIME ZAC, Instituto Politécnico Nacional, México 07738 D.F., México*

[3]*ESIQIE, Instituto Politécnico Nacional, México 07738 D.F., México*

[4]*Centro de Investigación en Ciencia Aplicada y Tecnología Avanzada Unidad Querétaro, Instituto Politécnico Nacional, Santiago de Querétaro, Querétaro, 76090, México*

[5]*Depto. Física y Matemáticas, Universidad Iberoamericana, Prol. Paseo de la Reforma 880, Lomas de Santa Fe, México 01219 D.F. México*

*Corresponding author: Carlos Torres Torres

Phone +52(55)57-29-60-00, ext. 54686

Fax +52(55)57-29-60-00, ext. 54587

*email: ctorrest@ipn.mx; crstorres@yahoo.com.mx

Abstract

The observation of photoconduction and nonlinear optical absorption on functionalized multi-wall carbon nanotubes decorated with platinum is reported. The samples were prepared by a chemical vapor deposition method. The electrical conductivity of the carbon nanotubes seems to be decreased by the functionalization process; but this property is strongly enhanced after the incorporation of platinum particles. Non-resonant photoconductive experiments at 532 nm and 445 nm wavelengths allow us to detect a selective participation of the platinum to the photoelectrical response. A mechano-optic effect based on Fresnel reflection was obtained through a photoconductive modulation induced by the rotation of a silica substrate where the samples were deposited as a thin film. A two-photon absorption process was identified as the main physical mechanism responsible for the nonlinear optical absorption. We consider that important changes in the nonlinear photon interactions with carbon nanotubes can be related to the population losses derived by phonons and the detuning of the frequency originated by functionalization.

Keywords: photo nanosystems; photoconduction; nonlinear optics; functionalization; chemical vapor deposition

1. Introduction

One of the most significant scientific interest related to study carbon nanostructures, comes from their particular advantages for designing nanosystems that can be improved by a number of materials [1]. Among some examples devoted to investigate high sensitive instrumentation of signals, diverse reports have been dedicated to describe mechanical [2-5] or electrical [6-8] tasks that highlight the extraordinary properties exhibited by carbon nanotubes (CNTs).

Several preparation methods for evaluating the morphological and structural characteristics of CNTs have been carried out [9,10]; and also, the possibility to influence the resulting physical functions of advanced materials based on CNTs seems to be attractive [11]. Moreover, it is notable that the adjustment of singular physical features during the processing route of different samples has been accomplished by implementing hybrid organic-inorganic materials mainly constituted by CNTs [12-15].

In many fields of nanotechnology, distinct kinds of CNTs have drawn considerable attention regarding their outstanding optical and electrical parameters [16,17]. In addition, the great importance of the third order optical nonlinearities of CNTs has also originated to consider them as exceptional materials for proposing all-optical systems displaying powerful absorptive and refractive nonlinear effects [18-22]. Apparently, the development of nonlinear low-dimensional compound materials is a crucial step towards the improvement of all-optical nanotechnology [23]. So, in regards to the fascinating mechanical, optical and electrical response associated to CNTs, an opportunity to use them for developing multi-functional smart materials can be contemplated.

The research progress of the photoconductive and mechano-optical response with CNTs and other metal elements have originated that different configurations can be considered as ideal candidates for next-generation of flexible transparent conducting films [24]. Decoration of CNTs by metallic nanoparticles (NPs) is attractive because the resulting physical characteristics exhibited by the individual components can be enhanced [25-27]. Using electrochemical deposition methods, a good control on size and densities of Pt NPs or bimetallic Pt-Ru NPs decorating CNTs has been accomplished [28,29]. On the other hand, microwave-assisted hydrothermal synthesis has allowed the preparation of Pd NPs, Ni NPs, and Sn NPs decorated on CNTs [30]. Following a polyol process, homogeneous distributions of Au NPs, Ag NPs, Pt NPs, Pd NPs, as well as bimetallic PtPd NPs and PtRu NPs, have been deposited on CNTs [31-35]. And it has been pointed

out that the optical transmittance and electrical conductivity of the resulting samples can be controlled by the deposition time of the processing route [35]. Moreover, in order to form heterojunctions of CNTs to metal NPs, eletron-beam systems have been employed [36-38], and Fe NPs, Co NPs, Ni NPs, and FeCo Nps, decorating CNT with improved electrical and mechanical properties have been obtained [39].

With this motivation, in this research an attempt has been made to further investigate the potential applications of the photoconductive and mechano-optic response of multiwall CNTs (MWCNTs). Experimental results associated to functionalization, electrical, photoconductive and nonlinear optical absorption phenomena that were successfully enhanced by platinum decoration of the studied samples are presented.

2. Experimental details

2.1. MWCNTs: synthesis and functionalization

MWCNTs were produced by thermal decomposition of Toluene (Fermont, 99.9% purity) and Ferrocene (Sigma-Aldrich, 98% purity) in a tubular reactor at T = 850 °C, P_{tot} = 80.1 kPa for 40 min. Ferrocene was dissolved in Toluene to form the source solution in a 1/39 mol ratio. The solution was nebulized as microdroplets and carried into the reactor by Ar gas with a flow rate of 2.5 L/min. [40]. MWCNTs were functionalized in 3:1 v/v mixture of sulfuric (30 mL, 95-97%) and nitric acid (10 mL, 65%) under sonication (42 kHtz) for 15 min at room temperature. After functionalization, MWCNTs were repeatedly washed in distilled water, centrifuged and dried in vacuum. [41]. The quality of functionalized MWCNTs (f-MWCNTs) was investigated by Raman Spectroscopy (Jobin Yvon Horiba).

2.2. Incorporation of metal NPs on f-MWCNTs

The f-MWCNTs decorated with platinum particles (Pt/f-MWCNTs) were prepared by an *in-situ* vapor-phase grafting process of Pt acetylacetonate [$(CH_3\text{-}COCHCO\text{-}CH_3)_2Pt$ Aldrich, 97%] in a quartz tube reactor at total pressure of 0.26 kPa. Pt-acac was decomposed in two sequential

thermal steps; the first at 180 °C for 600 s and the second at 400 °C for 600 s in a different reactor segment.

Afterwards, the resulting samples were suspended in an ethanol solution contained in a quartz cuvette with 1 mm width. The concentration of the solution was heuristically chosen for a better observation of the optical absorption bands that correspond to the plasmonic response of the samples in their linear optical spectra. Then, the obtained liquid solutions were deposited by dripping on different SiO_2 substrates, deriving in selected thin film samples with a resulting thickness of approximately 1 μm. The thin films were used for performing the electrical measurements and the nonlinear optical experiments.

2.3. Photoconductive measurements

Electrical measurements were evaluated using an Autolab/PGSTAT302N high power potentiostat/galvanostat. The impedance spectrum was measured with a 10 mV signal and an integration time of 1 s. The photoconduction on the samples was separately investigated at 445 nm and 532 nm wavelengths with continuous wave (CW) lasers providing 1 W of average power. The incident polarization of the optical beam was aligned to coincide with the path in measurement. The electrodes used for these experiments were in direct contact with the sample; they were located in the neighborhood of the diameter of the incident beam. The conductivity was measured using two metallic electrodes separated by a distance of 5 mm for each studied sample.

2.4. Linear optical response

The linear absorption spectrum of the samples was acquired with a Perkin Elmer XLS UV-visible spectrophotometer.

2.5. Photoconduction and nonlinear optical response

The optical transmittance and photoconduction in the thin films were measured by means of a high irradiance single beam transmittance experiment. A 532 nm wavelength with 1 ns pulse duration was monitored using the second harmonic of a Nd-YAG laser source Continuum Model SL II-10.

2.6. Mechano-optic regulation of photoconduction

Considering the possibility to promote controlled contributions of light for inducing a photoconduction behavior in the sample, we proposed the optoelectronic system assisted by a mechanical actuator illustrated in Fig. 1. The rotation of the sample generates a change in the

transmitted light through the SiO_2 substrate due to Fresnel reflection. So, the variation in the incident light on the Pt/f-MWCNTs allows a modification on the resulting photoconductive effect.

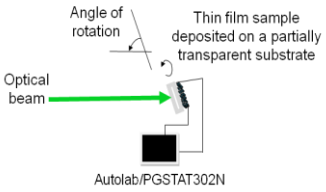

Figure 1. Setup for implementing a mechano-optic modulation of photoconduction.

3. Results and Discussion

Figure 2 shows the Raman spectra of the studied pristine and f-MWCNTs. Three characteristic peaks are clearly observed: the *D* band (~1334 cm^{-1}), the *G* band (~1580 cm^{-1}) and the *G´* band (~2660 cm^{-1}). The intensity ratio of the *D* and *G* bands ($I_{D/G}$) was estimated to be 0.68 for pristine MWCNTs and 0.38 for f-MWCNTs. As the *D* and *G* bands are indicative of defects and graphitic structure, respectively, the decrease in the $I_{D/G}$ ratio was interpreted as a reduction of defects in the f-MWCNTs. In addition, the increase in the *G*' band intensity for f-MWCNTs was consistently related to a decrement of defects and impurities [42].

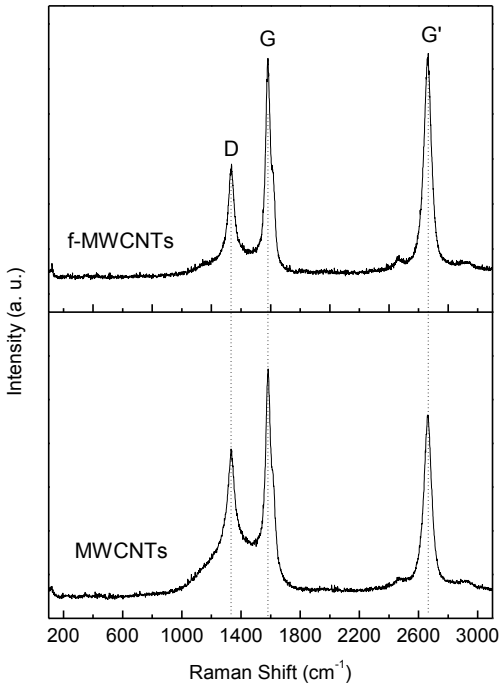

Figure 2. Raman spectra of pristine and functionalized nanotubes (f-MWCNTs).

A representative Field Emission Scanning Electron Microscopy (FE-SEM) image of Pt/f-MWCNTs is shown in Fig. 3. Pt particles are uniformly distributed on the external surface of nanotubes. In this sample, Energy-dispersive X-ray spectroscopy (EDX) analysis indicated that Pt content was about 5 wt. %. High Resolution Transmission Electronic Microscopy (HRTEM) observations (inset) reveled that Pt particles have a mean size of 2.3 nm.

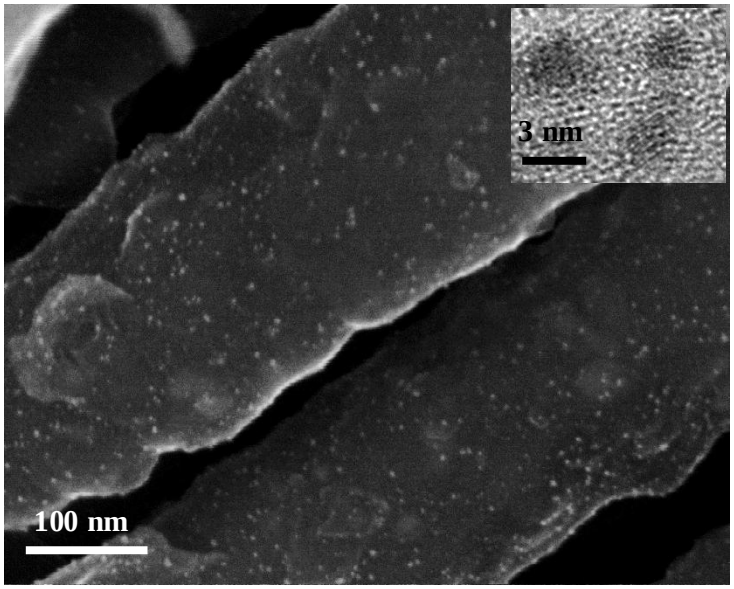

Figure 3. Field Emission-SEM image of Pt/*f*-MWCNTs.

It has been previously reported that the incorporation of Pt will increase the conductivity exhibited by decorated carbon nanotubes [43]. The electrical results for our studied samples are shown in Fig. 4. As it could be expected, a considerable enhancement in the resulting alternating current (AC) was derived from the incorporation of Pt in the nanotubes. But it is worth noting that the functionalization of the tubes originates a remarkable inhibition of the conductive response; probably because this process may promote the quenching of free holes that generates a change in the conductive phenomena.

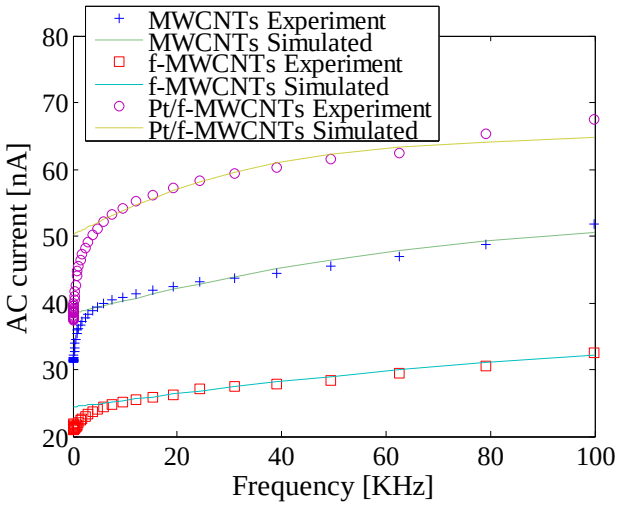

Figure 4. Electrical response of the studied samples as a function of electrical frequency.

Photoconductive results were obtained in darkness and under 532 nm wavelength of irradiation on the samples. The experimental data are presented in Fig. 5. While photoconduction was observed for the undecorated MWCNTs, no photoconduction was detected for the f-MWCNTs; but a redistribution of the charges in the resistive model together with a change in capacitance was present.

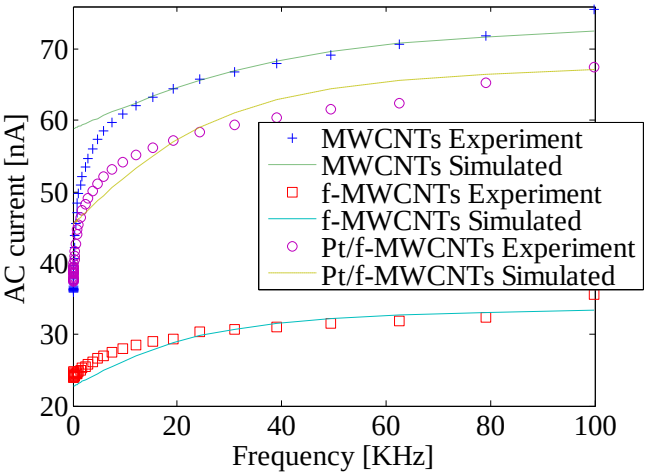

Figure 5. Photoconductive response under 532 nm irradiation as a function of electrical frequency.

Comparatively, photoconductive explorations carried out in the samples by a 445 nm irradiation seem to activate the photoconductive response in the f-MWCNTs as it can be observed from Fig. 6. An evident change in the electric signals can be observed by comparing the different conditions of photonic excitation.

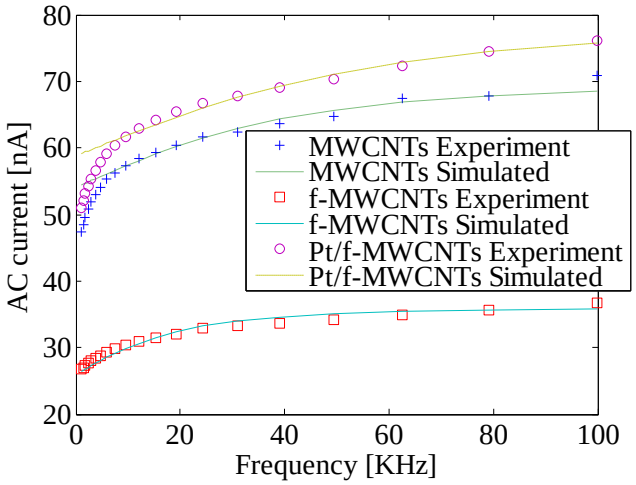

Figure 6. Photoconductive response under 445 nm irradiation as a function of electrical frequency.

The fitting of the experimental data shown in Figs. (4-6) were achieved by numerical simulations considering the Ohm's law and the following expression,

$$|Z| = \frac{R_1\sqrt{R^2 + {X_C}^2}}{R_1 + \sqrt{R^2 + {X_C}^2}}, \quad (1)$$

where, $X_C = {}^{-j}\!/_{\omega C}$, $j = \sqrt{-1}$, ω is the angular frequency of the AC of electrons; R and R_1 represent the electric resistances, X_C is the capacitive reactance and C is the capacitance. Best fitting parameters are presented in Table 1.

Table 1. Electrical parameters in the studied samples.

Experiment	**R_1 (Ω)**	**R (Ω)**	**C (pF)**
MWCNTs In darkness	260000	639594	3
MWCNTs Under 532nm irradiation	170000	659594	5
MWCNTs Under 445nm irradiation	185000	630000	5.5
f-MWCNTs	410000	809594	1.6

In darkness			
f-MWCNTs	899594	440000	6
Under 532nm irradiation			
f-MWCNTs	385000	1000000	7
Under 445nm irradiation			
Pt/f-MWCNTs	199000	639594	6
In darkness			
Pt/f-MWCNTs	220000	439594	11
Under 532nm irradiation			
Pt/f-MWCNTs	170000	500000	5
Under 445nm irradiation			

Taking into account the data described in Table 1, for the higher electrical frequencies plotted in Figs. (5) and (6), the photoconductive response in the Pt/f-MWCNTs shows a stronger capacitance behavior associated to the change in their monotonically increase in conductivity. This behavior is consistent with the fact that some electrical charges could be stored by the excitation of Pt ions that are also incorporated in the tubes. Regarding these photoconductive results, it can be considered that the functionalization ought to originate a modification of meta-stable electronic states that results in a decrease of the conductivity.

On the other hand, the experimental setup illustrated in Fig. 1 was implemented in order to explore the possibility for developing a mechano-optic sensor assisted by photoconduction. The response of the system was based on the photoconductive properties of the Pt/f-MWCNTs deposited on a SiO_2 substrate under a 445 nm irradiation with 1 W average power. In Fig 7 are plotted the experimental results acquired as a function on the angle of rotation.

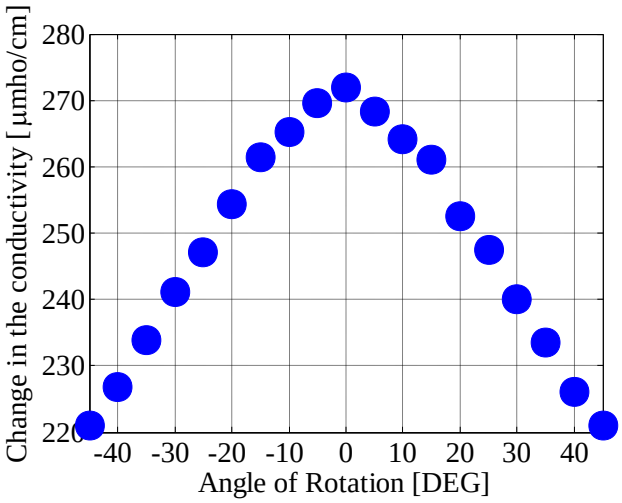

Figure 7. Photoconductive response in the studied Pt/*f*-MWCNTs as a function of the angle of rotation of the supporting substrate.

To better describe the contribution of multi-photonic interactions in the electrical measurements, a quantification of the linear and nonlinear optical response of the samples was undertaken. Similar optical spectra were obtained for studied samples with equivalent amounts of MWCNTs, f-MWCNTs or Pt/f-MWCNTs. Figure 8 depicts a representative linear absorption spectrum exhibited by the Pt/f-MWCNTs sample. One can clearly see at the plot, close to 270 nm wavelength, an absorbing band associated with the plasmonic response of the studied samples.

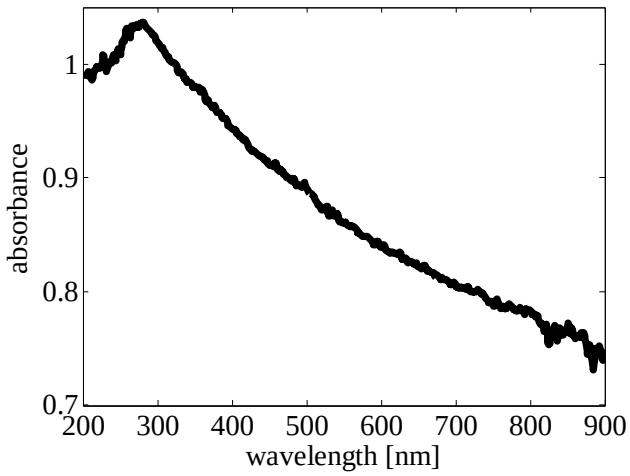

Figure 8. Linear optical absorption spectrum of Pt/*f*-MWCNTs.

A high irradiance optical beam at 532 nm wavelength was selected to observe if any involvement of multi-photonic interaction could be discerned during the propagation of a non-resonant optical beam. Figure 9 illustrates the obtained results; a noticeable modification in the transmittance for the Pt/f-MWCNTs can be clearly distinguished.

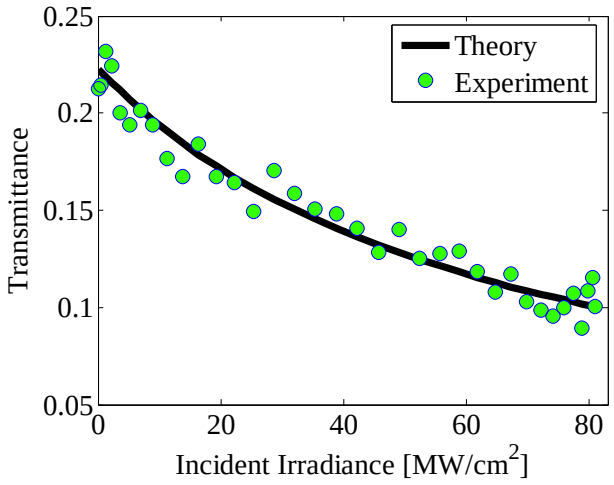

Figure 9. Nonlinear optical transmittance exhibited by Pt/*f*-MWCNTs.

The fit of the nonlinear optical transmittance was performed using the expression for the transmitted irradiance *I(L)* in the presence of nonlinear optical absorption:

$$I(L) = \frac{I_o \exp(-\alpha_o L)}{1 + \beta I_o L_{eff}}, \tag{2}$$

where β represents the nonlinear absorption coefficient; I_o is the total irradiance of the incident beam, L_{eff} is the effective length given by $L_{eff} = \left(1 - e^{-\alpha_o L}\right) / \alpha_o$, with L the sample length, and α_o the linear absorption coefficient.

The best fitting for the linear and nonlinear absorptive coefficients for the samples results in α_0 = 15 cm^{-1} and β = 1.51×10^{-7} cm/W for the Pt/f-MWCNTs case. The error bar in the experimental data is around ±5%. A typical behavior of a two-photon absorption (TPA) effect in Pt/f-MWCNTs is evidently described by the transmittance results plotted in Fig. 9. This TPA phenomenon, together with the enhancement in the photoconductivity at higher repetition rates of nanosecond pulses, could be associated with an important contribution of multi-photonic interactions that results after the incorporation Pt in the tubes.

In order to explain the observed nonlinear optical response, we considered the dipole approximation in a system of N two-level atoms per unit volume under a high optical irradiance. Then, in the limit of large detunings, i.e., $T_2\Delta >> 1$, it can be demonstrated that the real and imaginary part of the third order optical susceptibility, $\chi^{(3)}$, can be written as [44,45],

$$\mathrm{Re}\,\chi^{(3)} \approx \frac{4}{3} N m^4 \left[\frac{1}{\hbar\Delta}\right]^3 \frac{T_1}{T_2}\,, \tag{3}$$

$$\mathrm{Im}\,\chi^{(3)} \approx -\frac{4}{3} N m^4 \left[\frac{1}{\hbar\Delta}\right]^3 \frac{T_1}{T_2^2\Delta}\,, \tag{4}$$

where *m* represents the atomic dipole moment, $\Delta=\omega-\omega_{21}$ is the detuning of the frequency ω of the incident radiation, $1/T_1$ represents the population loss through radiative and non-radiative processes of the upper level, and $1/T_2$ represents the rate of polarization loss for the off-diagonal matrix elements. From Eqs. (3) and (4) it is possible to observe an evident influence of the temporal radiative and non-radiative processes on the third order optical response. Under non-resonant conditions, the non-radiative spontaneous emission of the atoms would be much smaller than both the radiative spontaneous emission, nevertheless, a modification in the optical nonlinearities is expected for important changes in the nonlinear photon interactions mainly related to the population losses derived by phonons and the detuning of the frequency originated by functionalization.

For further investigate the participation of optical absorption in the physical mechanism responsible of the photoconductivity, we irradiated the samples by employing optical pulses at 532 nm with about 50 MW/cm^2 at 1 Hz repetition rate provided by our Nd-YAG system. The data shown in Fig. 10 correspond to 5 optical pulses and the results point out an important change in the photoconduction dependent on the incident pulses. Experimental observations compared to previous reports [46] reveal that a noticeable participation of a thermal effect could be expected to activate an additional conductive effect into our samples as it can be seen from Fig 10.

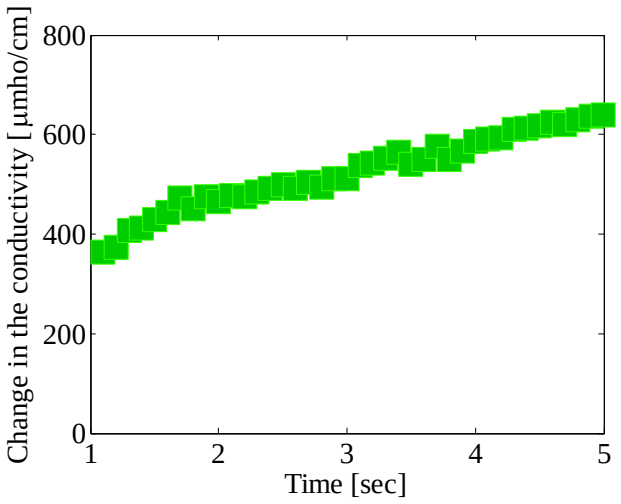

Figure 10. Photoconductive response dependent on nanosecond irradiation in Pt/*f*-MWCNTs.

We calculated the heat-transference generated by optical irradiation in propagation through the sample by using [47],

$$\frac{\partial T}{\partial t} = \frac{\partial}{\partial z}\left[\frac{\kappa}{\rho C}\frac{\partial T}{\partial z}\right] + \frac{\alpha}{\rho C} I(t,z), \tag{5}$$

here T is the temperature, which is a function of the estimated depth in our sample z=1 μm. As a first approximation, we considered the thermal conductivity κ= 200 W/mºK, the density ρ= 1×10^{-3} Kg/cm^3, and the heat capacity C=1×10^3 J/KgºK for MWCNTs previously reported [48]. In our case the time of irradiation t= 5 s, the linear absorption coefficient α=2×10^6 m^{-1} and I the optical intensity. The estimated results indicate that an instantaneous temperature change of approximately 180º K can be expected after the propagation of each pulse. However experimental measurements allow us to state that long duration temperature changes (after at least one second) of about 2º K were detected in agreement with our calculations.

The possibility to enhance the nonlinear optical response and the electronic features of CNTs samples by the modification of meta-stable electronic levels appears to be attractive. What is more, we consider that potential applications for tailoring the optical and the electrical response associated to diverse materials can be also improved by the incorporation of NPs capable to change electrical and optical interactions. Regarding the contribution of the absorptive nonlinearities to the electrical properties of the studied samples, potential applications for developing optoelectronic nanosystems based on decorated CNTs can be contemplated.

4. Conclusion

A noticeable enhancement in the electrical and photoconductive response exhibited by f-MWCNTs nanotubes was achieved by platinum decoration. Apparently, the incorporation of platinum NPs on MWCNTs originates a modification in the non-resonant electronic levels that can play an important role in the resulting photoconductive and two-photon absorption effects. A simple mechano-optic effect based on the photoconductive response exhibited by the studied samples was observed.

Acknowledgments

The authors kindly acknowledge the financial support from the Instituto Politécnico Nacional, Universidad Iberoamericana and CONACyT. The authors are also thankful to the Centro de Nanociencias y MicroNanotecnologías-IPN.

References

[1] A. Karina Cuentas-Gallegos, R. Martínez-Rosales, M.E. Rincón, G.A. Hirata, G. Orozco, Optical Materials, 29 (2006) 126-133.

[2] F. Galantini, S. Bianchi, V. Castelvetro, G. Gallone, Smart Mater. Struct. 22 (2013) 05505.

[3] J. N. Coleman, U. Khan, W. J. Blau, J. K. Gun'ko, Carbon 44 (2006) 1624-1652.

[4] D. Carey, J. Electron. Mater. 17 (2006) 397-398.

[5] E. Feria-Reyes, C. Torres-Torres, H. Martínez-Gutiérrez, S. Morales-Bonilla, R. Torres-Martínez, M. Trejo-Valdez, G. Urriolagoitia-Calderón, "Mechano-optical modulation and optical limiting by multiwall carbon nanotubes,", J. Mod. Optic, 60(16), (2013) 1321-1326.

[6] K. Fujisawa, T. Tojo, H. Muramatsu, A. L. Elías, S. M. Vega-Díaz, F. Tristán-López, J. H. Kim, T. Hayashi, Y. A. Kim, M. Endo, Nanoscale 3 (2011) 4359-4364.

[7] J. M. Romo-Herrera, M. Terrones, H. Terrones, V. Meunier, ACS Nano 2 (2008) 2585-2591.

[8] N. E. Gorji and G. Xosrovashvili, Int. J. Photoenergy (2014) in press.

[9] J. H. Lehman, M. Terrones, E. Mansfield, K. E. Hurst, V. Meunier, Carbon 49 (2011) 2581-2602.

[10] D.H. Galvan, A. Aguilar-Elguézabal, G. Alonso, Optical Materials, 2 (2006) 140-143.

[11] R. Reza, K. Jae-Kyung, N. Hani, Smart Mater. Struct. 18 (2009) 104002.

[12] F. Liu, X. B. Zhang, D. Häussler, W. Jäger, G. F. Yi, J. P. Cheng, X. Y. Tao, Z. Q. Luo, S. M. Zhou, J. Mater Sci 41 (2006) 4523-4531.

[13] B. Wu, Y. Kuang, X. Zhang, J. Chen, Nano Today 6 (2011) 75-90.

[14] T. Koretsune, S. Saito, Sci. Technol. Adv. Mater. 9 (2008) 044203.

[15] U. K. Gautam, P. M. F. J. Costa, Y. Bando, X. Fang, L. Li, M. Imura, D. Golberg, Sci. Technol. Adv. Mater 11 (2010) 054501.

[16] M. A. Mohamed, N. Inami, E. Shikoh, Y. Yamamoto, H. Hori, A. Fujiwara, Sci. Technol. Adv. Mater. 9 (2010) 025019.

[17] P. Rima, A. Maity, A. Mitra, P. Kumbhakar, A. K. Mitra, J. Nanopart. Res. 13 (2011) 5749-5757.

[18] R. Sreeja, P. M. Aneesh, K. Hasna, M. K. Jayaraj, J. Electrochem. Soc. 158 (2011) K187.

[10] K. C. Jena, P. B. Biskt, M. M. Shaijumon, S. Ramaprabhu, Opt. Commun. 273 (2007) 153-158.

[20] V. A. Margulis, O. V. Boyarkina, E. A. Gaiduk, Opt. Commun. 249 (2005) 339-349.

[21] C. Torres-Torres, N. Peréa-López, H. Martínez-Gutiérrez, J. Ortíz-López, M. Trejo-Valdez, Terrones, Nanotechnol 24 (2013) 045201.

[22] N. Izard, P. Billaud, D. Riehl, E. Anglaret, Opt. Lett. 30 (2005) 1509-1511.

[23] R. Torres-Torres, Electron. Lett., (2011) 47, 191-193.

[24] K. Wen-Yin, L. Kuan-Jiuh, J. Nanomat.,Vol. 2013, Article ID 505292, 16 pages.

[25]Y.-A. Li, N.-H. Tai, S.-K. Chen, and T.-Y. Tsai, ACS Nano, vol. 5, no. 8, pp. 6500–6506, 2011.

[26] Y. Lin, K. A. Watson, M. J. Fallbach et al., ACS Nano, vol. 3, no. 4, pp. 871–884, 2009.

[27] S. Sahoo, S. Husale, S. Karna, S. K. Nayak, and P. M. Ajayan, Journal of the American Chemical Society, vol. 133, no. 11, pp. 4005–4009, 2011.

[28]Z. He, J. Chen, D. Liu, H. Zhou, and Y. Kuang, Diamond and Related Materials, vol. 13, no. 10, pp. 1764–1770, 2004.

[29] Z.He, J. Chen,D. Liu,H.Tang, W. Deng, and Y. Kuang, Materials Chemistry and Physics, vol. 85, no. 2-3, pp. 396–401, 2004.

[30] T. Ramulifho, K. I. Ozoemena, R. M. Modibedi, C. J. Jafta, and M. K. Mathe, Electrochimica Acta, vol. 59, pp. 310–320, 2012.

[31] C.-Y. Lu, M.-C.Wei, S.-H. Chang, andM.-Y.Wey, Applied Catalysis A, vol. 354, no. 1-2, pp. 57–62, 2009.

[32] O. Winjobi, Z. Zhang, C. Liang, and W. Li, Electrochimica Acta, vol. 55, no. 13, pp. 4217–422, 2010.

[33] L. Li and Y. Xing, Journal of Physical Chemistry C, vol. 111, no. 6, pp. 2803–2808, 2007.

[34] L. Qiu, V. G. Pol, Y.Wei, and A. Gedanken, New Journal of Chemistry, vol. 28, no. 8, pp. 1056–1059, 2004.

[35] W.-Y. Ko, J.-W. Su, C.-H. Guo, and K.-J. Lin Carbon, vol. 50, no. 6, pp. 2244–2251, 2012.

[36] M. Terrones, H. Terrones, F. Banhart, J.-C. Charlier, and P. M. Ajayan, Science, vol. 288, no. 5469, pp. 1226–1229, 2000.

[37] F. Banhart Nano Letters, vol. 1, no. 6, pp. 329–332, 2001.

[38] C. Jin, K. Suenaga, and S. Iijima, Nature Nanotechnology, vol. 3, no. 1, pp. 17–21, 2008.

[39] J. A. Rodriguez-Manzo, F. Banhart, M. Terrones et al., Proceedings of the National Academy of Sciences of the United States of America, vol. 106, no. 12, pp. 4591–4595, 2009.

[40] R. Andrews, D. Jaques, A. M. Rao, F. Derbyshire, D. Qian, X. Fan, E. C. Dickey, J. Chen, Chem. Phys. Lett. 303 (1999) 467-474.

[41] A. Hirsch, O. Vostrowsky, Top Curr. Chem. 245 (2005) 193-237.

[42] R. O. DiLeo, B. J. Landi, R. P. Rafaelle, J. Appl. Phys. (2007) 101 064307.

[43] C. Mercado-Zúñiga, J. R. Vargas-García, F. Cervantes-Sodi, M. Trejo-Valdez, R. Torres-Martínez, C. Torres-Torres, Appl. Optics 52 (2013) E22-E27.

[44] V. Yannopapas, Opt. Commun. 283 (2010) 1647-1649.

[45] M. Trejo-Valdez, C. Torres-Torres, J. H. Castro-Chacón, G. A. Graciano-Armenta, C. I. García-Gil, A. V. Khomenko, Opt. Laser Technol. 49 (2013) 75-80.

[46] W. M. Jacobs, D. A. Nicholson, H. Zemer, A. N. Volkov, L. V. Zhigilei, Phys. Rev. B 86 (2012) 165414.

[47] VonAllmen M., Blatter A., Laser–beam interaction with materials, Springer, Berlin 1995.

[48] Da Jiang Yang, Qing Zhang, George Chen, S. F. Yoon, J. Ahn, S. G. Wang, Q. Zhou, Q. Wang, J. Q. Li, Phys. Rev. B 66 (2002) 165440.